

Impact of water repellent agent concentration on the effect of hydrophobization on building materials

Chi Feng^{1,2,*}, Hans Janssen³

1. School of Architecture and Urban Planning, Chongqing University, 400045 Chongqing, PR China
2. Key Laboratory of New Technology for Construction of Cities in Mountain Area, Ministry of Education, Chongqing University, 400045 Chongqing, PR China
3. KU Leuven, Department of Civil Engineering, Building Physics and Sustainable Design, 3001 Leuven, Belgium

Abstract: It is desirable to avoid or lessen moisture-related problems in building components exposed to wind-driven rain via correct material design and/or choice. In some cases however – e.g. for historic building facades – the only possibility is to modify the hygric properties of existing materials. Hydrophobization treatment is suggested as a possible protocol, but the proper concentration of the water repellent agent to achieve the expected effect is still open to discussion. This study proposes the novel concept of a material-dependent critical agent concentration: the lowest concentration that ensures hydrophobic effectiveness on a specific material. For validation, the hygric impact of hydrophobization treatment at different agent concentrations is studied. Specifically, a balanced mixture of silanes and siloxanes is used as the agent, and eight experiments are performed on ceramic brick, lime mortar and sintered glass. Results demonstrate the existence of a material-dependent agent concentration. Only when treated above it will the hygric properties be significantly modified. Moreover, hydrophobization impacts the capillarity of a material much more than its hygroscopicity, due to the difficulty for the large molecules of water repellent agents to penetrate into fine pores. The bulk density, open porosity and pore size distribution are typically only minimally influenced.

Keywords: porous building material; hygric property; hydrophobization; critical agent concentration; pore size

1. Introduction

1.1 Background

According to the statistics of the International Energy Agency, buildings are in the top three energy-consuming sectors in the world, with an annual consumption of about 1200~1300 million tons of oil equivalent since 2000 [1]. It is hence of great importance to improve the energy efficiency of buildings. Of all the energy consumed by buildings, heating is responsible for a significant share [2, 3], and better envelope insulations are therefore necessary.

Generally speaking, the insulation of building envelopes can be classified into the external and the internal solutions. Although external insulation is often more optimal [4, 5], internal insulation remains the only choice in many situations, particularly for the thermal retrofitting for historic buildings whose exterior facades must be preserved [6, 7]. Application of internal insulation lessens buildings' energy consumption and improves the indoor thermal comfort. However, internal insulation also significantly changes the hygrothermal characteristics of building envelopes and hence may give rise to interstitial condensation [8], frost damage [9], mould growth [10] and other moisture related challenges [11].

The main reasons for these moisture-related problems in internally insulated facades are their easy moisture absorption (especially from wind-driven rain [12-14]) versus the reduced drying potential of

*Corresponding author: fengchi860602@gmail.com

Tel: +86 13240305046

the facade. Broadly speaking, switching to better-designed materials is a fundamental solution [15, 16]. In some cases though – e.g. for historic buildings – that option does not exist. The only possibility is to modify the hygric properties of existing porous building materials. For this reason, hydrophobization treatment has been raised as a protocol. It treats the external facade with a water repellent agent so that the hygric properties of the material are modified, preventing the facade from absorbing liquid water without significantly compromising its drying capability through vapor diffusion, hence resolving or at least relieving such moisture-related problems [12, 17].

1.2 Hydrophobization in brief

Hydrophobization is most widely applied as post-treatment on internally insulated historic buildings, thus current studies at the material level focus on brick and mortar, which compose the facades of these buildings. These materials can easily absorb liquid water due to the joint polarity of their pore surfaces and water molecules. After hydrophobization, the polar “heads” of the water repellent agent’s molecules are adhered to the pore surfaces of the building materials, while their non-polar “tails” raise the contact angle between water molecules and pore surfaces, subsequently preventing the spontaneous water absorption [18, 19]. As the agent does not completely block the pores of building materials, it is still possible for building envelopes to dry out through vapor diffusion [20].

There are different types of water repellent agents, like silicon-bearing compounds, metal-bearing compounds, or organic materials [18]. More recently nanotechnology-based agents have also been developed [21, 22]. Of all the commercially available agents, the silicon-bearing products are the most popular, enjoying a more than 80% share of the market [23]. They all contain a silicon-oxygen backbone but are often grouped into silanes, siloxanes and silicon resins, differing in their specific molecular structures [24].

Upon usage, the concentrated water repellent agent should be diluted, normally to a concentration suggested by the producer. Undoubtedly, different concentrations are needed for various agents to achieve effectiveness [12]. However, it is also true that different materials require different concentrations of the same agent [23, 25, 26], as their varied open porosities and pore size distributions lead to distinct pore surface areas. Unfortunately, current recommendations from the producers fail to differentiate the necessity of different materials, and a single over-estimated concentration of one agent is often recommended for all materials. Although this approach guarantees the effectiveness of hydrophobization, it is not optimal in economic, environmental and even health-related aspects.

1.3 Objectives

This study experimentally investigates the balance between the water repellent agent’s concentration and its hydrophobizing effectiveness. By proposing the novel concept of a material-dependent critical agent concentration, the lowest concentration that ensures a dependable hydrophobic effectiveness on different materials is identified. In the following sections, the target materials and the tests on hygric properties are introduced first. After that, the experimental results are presented in detail and analyzed in depth. Finally, our experimental results are confronted with measurements from literature for further discussion, and the concept of the critical agent concentration is proposed.

2. Materials and methods

In this section, we first introduce the target materials chosen for the tests and the procedures to perform the hydrophobization treatment. Next, the test protocols are briefly described. After that, the experimental arrangement is explicitly explained.

2.1 Materials

As explained before, ceramic brick and lime mortar compose many historic buildings' facades and are therefore chosen as target materials. Specifically, the brick used is Vandersanden Robusta brick [27], an industrial product widely used in Europe with good homogeneity. The mortar is on the other hand home-made, composed at the ratio of 10 liters of water, 12.5 kg of lime (Saint-Astier NHL3.5 [28]) and 50 kg of river sand (0/ 2 mm), with a moisture curing period of two months (ambient RH>98%) and an accelerated carbonation period of one month (in a carbonation chamber at 4.7% CO₂ concentration). Next to ceramic brick and lime mortar, ROBU VitraPOR[®] P100 sintered glass filter product [29] is also chosen as a target, even though it is not a real building material. It features superb homogeneity and relatively large pore sizes. We expect that the critical agent concentration depends heavily on the pore size of a material, thus sintered glass is also included to provide additional information.

2.2 Hydrophobization treatment

The hydrophobization treatment is carried out with the agent SILRES[®] BS SMK 2100, a solventless silicone microemulsion concentration. It has a balanced mixture of silanes and siloxanes at a ratio of roughly 50/50. Its exact composite is proprietary and hence not publicly available, but this is not indispensable to investigate and exemplify the concept of material-dependent critical agent concentrations.

Upon usage, the producer recommends diluting the concentrated agent with water to a volumetric concentration of around 10%, for both brick and mortar [30]. To screen for the minimal effective concentration, the concentrated agent is diluted down to 10%, 0.1% and 0.01% in this study. After that, samples of different materials absorb these diluted solutions via a capillary uptake process until the agent reaches the samples' top surfaces. Next, samples are cured at 100% ambient RH for two weeks and at 54% for another week. Finally, they are dried in a ventilated oven at 70°C. This treatment differs from the in-situ procedures but is recommended by the producer for laboratory studies.

It should be mentioned that all three materials have been treated at 10% and 0.1% agent concentrations. Ceramic brick, the typical large-pore material for historic buildings, has a smaller pore surface area than mortar. Hence a lower agent concentration may be sufficient for ceramic brick, and 0.01% is also included for it in some tests.

2.3 Test Methods

As summarized in Table 1, in total eight different measurements are performed to determine material properties. Most of these methods have been standardized, and their specific operational procedures are not reiterated; only the key information is provided. For the drying test – not being a standard test – more details are provided.

Table 1 Test methods and corresponding material properties

	Test	Reference standard	Obtained property
Basic tests	Vacuum saturation test	ISO 10545 [31]	$\rho_{bulk}, \phi, w_{sat}$
	Mercury intrusion test	ASTM D4404 [32]	Pore volume distribution
Storage tests	Desiccator test	ISO 12571 [33]	Sorption isotherms
	Pressure plate test	ASTM C1699 [34]	Moisture retention curve
Transport tests	Capillary absorption test	ASTM C1794 [35]	A_{cap}, w_{cap}
	Water head test	ISO 17892-11 [36]	K_l
	Cup test	ISO 12572 [37]	μ
	Drying test	-	μ

2.3.1 Basic tests

The vacuum saturation test is performed to determine the bulk density (ρ_{bulk} , $\text{kg}\cdot\text{m}^{-3}$), open porosity (ϕ , -) and saturated moisture content (w_{sat} , $\text{kg}\cdot\text{m}^{-3}$). Since w_{sat} is linearly related to ϕ with water density as the coefficient, only one of them (ϕ) is reported and discussed in the following analysis.

Mercury intrusion porosimetry is performed to obtain the pore volume distribution, expressed as the volume fraction for pores of different radii ($f_v(r)$, %). This test is influenced by many factors (such as the choice of the contact angle) and is not reliably repeatable [38-40], so we refer to its results mainly for relative comparison.

2.3.2 Moisture storage tests

In the hygroscopic range, the desiccator test is performed to get the gravimetric moisture content (u , $\text{kg}\cdot\text{kg}^{-1}$) – which is needed for fitting sorption isotherms – at seven different RHs, including 11.3%, 32.9%, 53.5%, 75.4%, 84.7%, 94.0% and 97.4%. Saturated salt solutions are used for humidity control.

In the over-hygroscopic range, the pressure plate test is performed to acquire the data point for the moisture retention curve. The applied air pressures include $1.25\cdot 10^4$, $2.5\cdot 10^4$, $5\cdot 10^4$, $1\cdot 10^5$, $1.5\cdot 10^5$, $2\cdot 10^5$, $3\cdot 10^5$, $5\cdot 10^5$, $7\cdot 10^5$, $1\cdot 10^6$ and $1.5\cdot 10^6$ Pa, but not all samples have gone through these pressures due to their different moisture retention characteristics.

It should be mentioned that for the storage measurements, hydrophobized samples are always pre-conditioned to w_{sat} for the desorption process, while desorption from the capillary moisture content (w_{cap} , $\text{kg}\cdot\text{m}^{-3}$) is also included for untreated samples. In the hygroscopic range, the adsorption isotherms starting from the dry state are also tested on untreated samples.

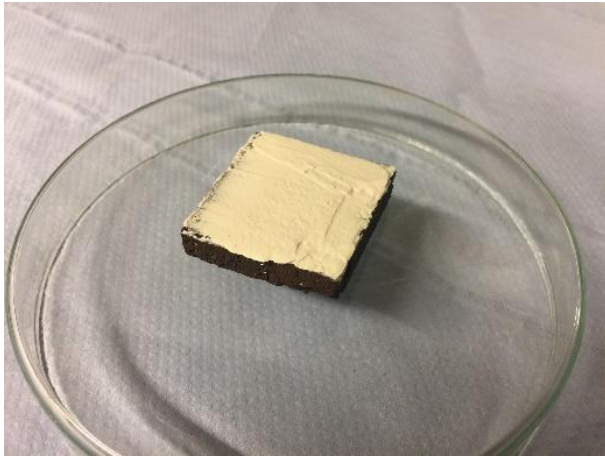
2.3.3 Moisture transport tests

The capillary absorption test is performed for the capillary absorption coefficient (A_{cap} , $\text{kg}\cdot\text{m}^{-2}\text{s}^{-0.5}$) and w_{cap} . For hydrophobized samples the water front sometimes fails to reach the top even after an elongated test period, thus w_{cap} is not always available.

The water head test is performed to derive the liquid permeability (K_l , $\text{kg}\cdot\text{m}^{-1}\text{s}^{-1}\text{Pa}^{-1}$). There are both constant-head and falling-head versions [41-43], and in this study we use a modified falling-head setup. The falling water head involves transient flow, causing complexity in data processing. In the Appendix we elaborate the calculation method. Note that due to its working principle, this falling water head test is only applicable to a moisture content (w , $\text{kg}\cdot\text{m}^{-3}$) between w_{sat} and w_{cap} .

The cup test is performed to assess the vapor permeability, expressed as the vapor diffusion resistance factor (μ , -). Saturated salt solutions are used to impose the three RH conditions: 11.3%~53.5%, 53.5%~84.7% and 84.7%~97.4%.

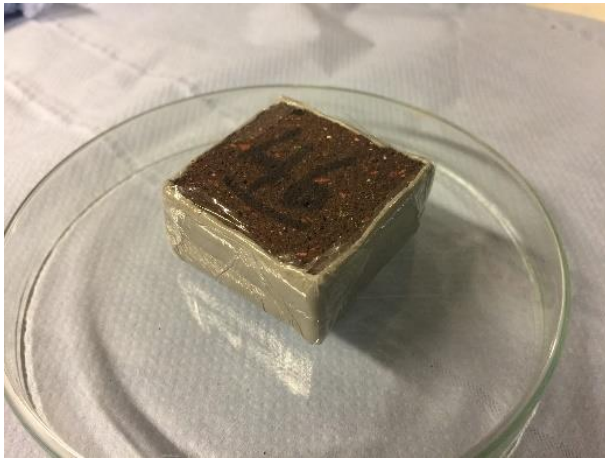
The drying test, finally, is performed to get the moisture transport coefficient, also expressed as the moisture transport resistance factor (μ , -). Fig. 1 depicts the experimental procedures. First, a thin layer of kaolin is laid on top of an untreated sample pre-conditioned to w_{sat} . Next, another sample of the same size, either untreated or treated, is laid above the kaolin. After that the bottom and the lateral sides of these two samples are sealed. Finally, the samples are put in a climate chamber for 1-D drying. The bottom of the upper sample is assumed to have an RH of 100% because it contacts the saturated sample through kaolin, while the ambient RH in the climate chamber is known (84% in this study). By checking the drying rate, the equivalent moisture transport resistance factor of the upper sample can be derived, with the help of the sample's dimension. Unlike the cup test where vapor contact is the only boundary condition, the drying test involves the contact with the underlying wet sample to promote liquid transfer. Consequently, this test is an important complement to the cup test, explicitly focusing on the identification of remaining liquid transfer.



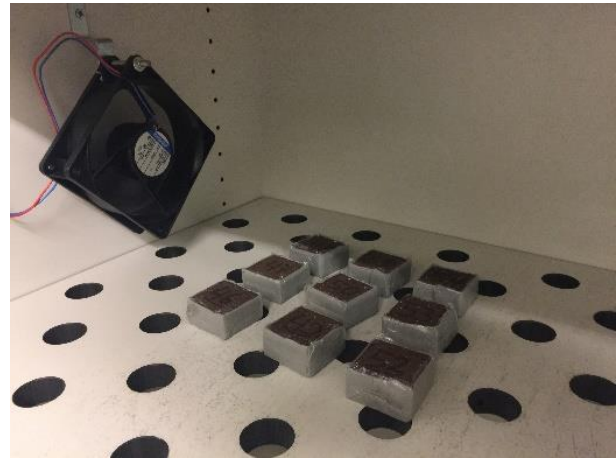
a. Kaolin and saturated sample



b. (Un)treated sample above the kaolin



c. Bottom and lateral sealing



d. Drying process

Fig. 1 The procedures of the drying test

2.4 Experimental arrangement

All measurements are carried out at 22~23°C. Except for the mercury intrusion test where a single sample is used, all other tests employ 3 to 5 replicate samples. Obviously, it is a very time- and energy-consuming task to conduct all the above-mentioned tests on all treated and untreated materials. As explained in the next section, it is also unnecessary to complete them all. Consequently, some measurements are omitted, resulting in the experimental arrangement in Table 2.

Table 2 The experimental arrangement

Material		Ceramic brick		Lime mortar		Sintered glass	
		Yes	No	Yes	No	Yes	No
Basic tests	Vacuum saturation test	√	√	√	√	√	√
	Mercury intrusion test	√	√	√	√	√	√
Storage tests	Desiccator test	-	√	√	√	-	-
	Pressure plate test	√	√	√	√	√	√
Transport tests	Capillary absorption test	√	√	√	√	√	√
	Water head test	√	√	√	√	√	√
	Cup test	√	√	√	√	-	-
	Drying test	√	√	√	√	-	-

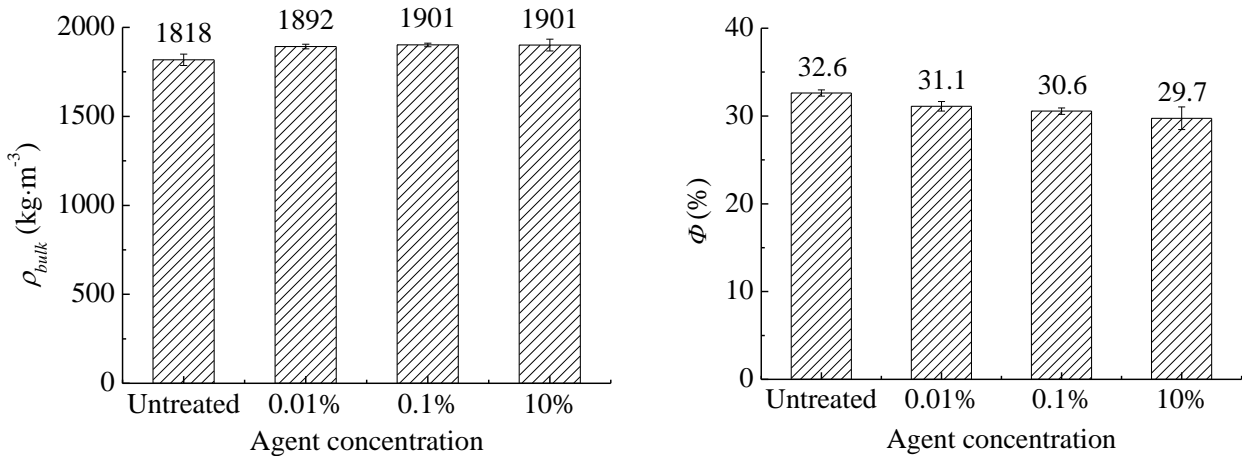
3. Results

In this section, the properties of treated and untreated target materials are reported and analyzed. These properties are presented in the basic-storage-transport order, as established in Section 2.

3.1 Results from basic tests

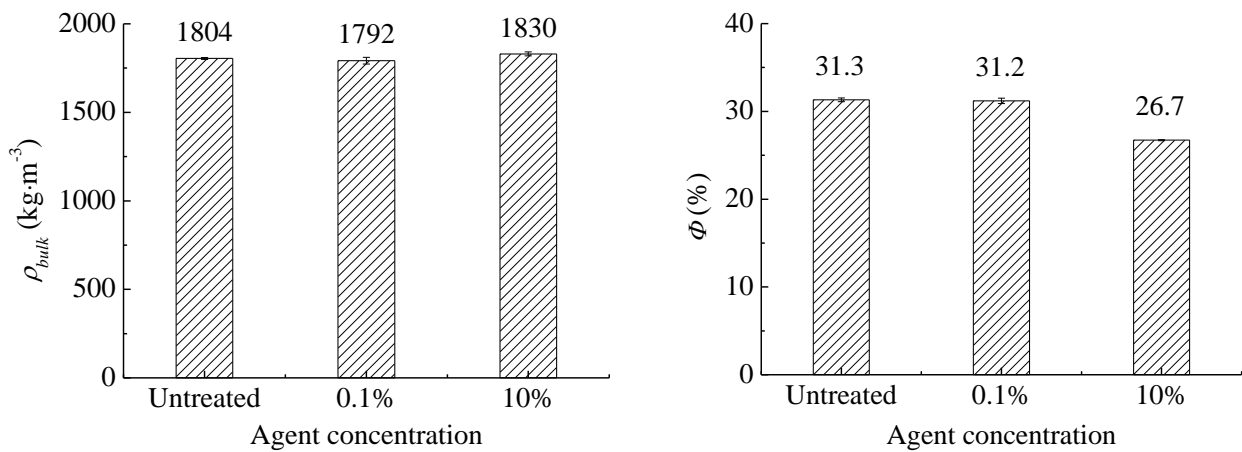
The bulk densities and open porosities obtained from the vacuum saturation tests are illustrated in Fig. 2, with error bars representing the standard deviations for multiple samples. The open porosity is decreasing with increasing agent concentration. This should be attributed to (partial) blocking of small pores by the water repellent agent, transforming some previously connected pores into isolated pores, resultantly reducing the open porosity. The effect remains minor however, as the reduction in porosity is limited to some 3%-4 % in absolute terms. The bulk density on the other hand exhibits no clear trend with agent concentration. Although ceramic brick and sintered glass demonstrate a slightly increasing bulk density with increasing agent concentration, lime mortar displays irregularities. The impact of the deposited agent on the total weight is small, and can thus be easily obscured by experimental variations.

The pore volume distributions obtained from mercury intrusion are illustrated in Fig. 3. Obviously, hydrophobization has a very limited impact on the overall pore volume distributions, for all three materials. Lime mortar shows some fluctuations in the 10^{-7} ~ 10^{-8} m pore-size region, as well as a very slight shift towards smaller pores after hydrophobization. Both phenomena should be mainly attributed to experimental and data processing uncertainties, as mercury intrusion tests are not reliably repeatable all the time [38-40]. Irregularities from this test are also observed in other measurements [44, 45].



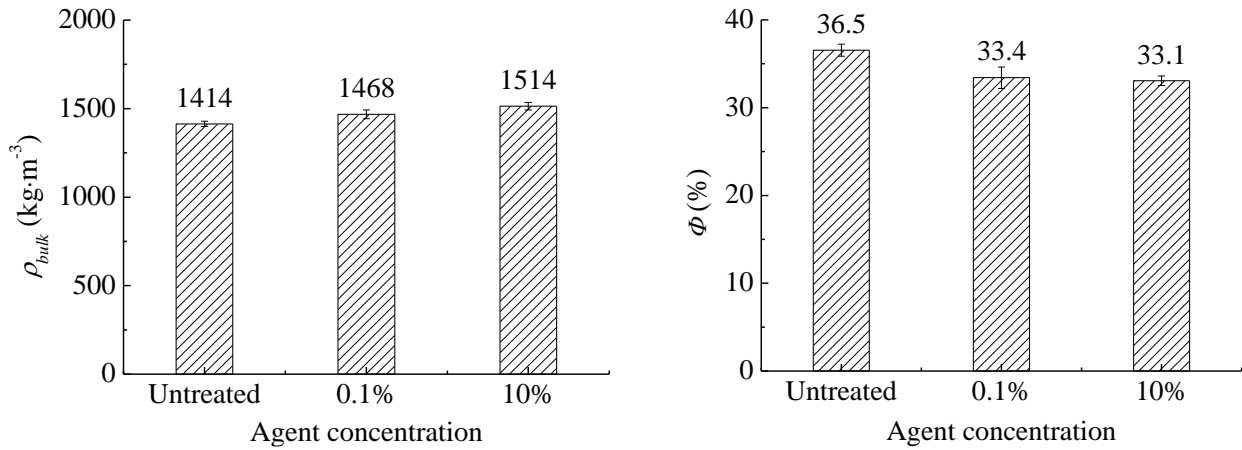
a. The bulk density of ceramic brick

b. The open porosity of ceramic brick



c. The bulk density of lime mortar

d. The open porosity of lime mortar



e. The bulk density of sintered glass
 f. The open porosity of sintered glass
Fig. 2 The bulk densities and open porosities obtained from the vacuum saturation tests

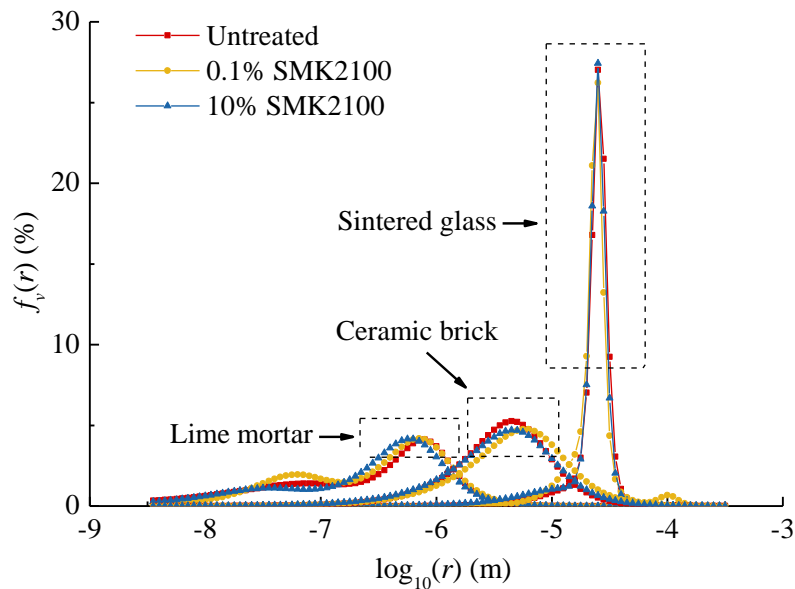


Fig. 3 The pore volume distribution obtained from the mercury intrusion tests

Summarized from the basic tests, it can be concluded that hydrophobization has a very moderate influence on the pore structures and the related properties of porous building materials. The concentration of the water repellent agent does not play a significant role here.

3.2 Results from moisture storage tests

The sorption isotherms obtained from the desiccator tests are illustrated in Fig. 4. For ceramic brick, trial measurements are first performed on untreated samples for both adsorption from the dry state and desorption from w_{sat} . Due to the material's weak hygroscopicity, the experimental uncertainties are too large however, so that the results are not reliable, deviating significantly from the expected smooth "S-shape" curves for most porous building materials. It is therefore also meaningless to test hydrophobized samples. As explained before, sintered glass is even less hygroscopic than ceramic brick. Consequently, it is neither tested for sorption.

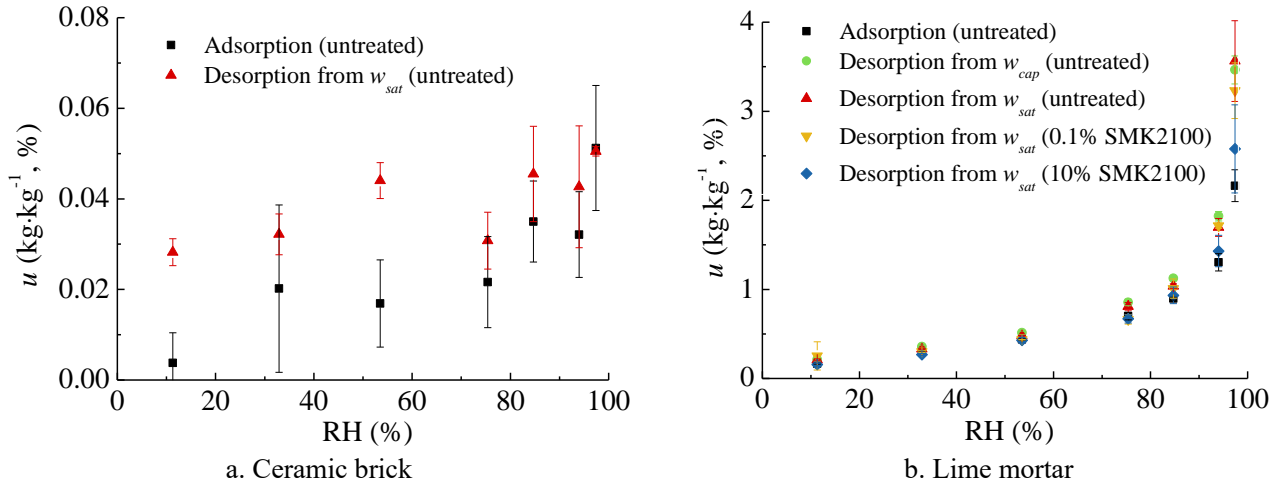


Fig. 4 The sorption isotherms obtained from the desiccator tests

For lime mortar, the sorption isotherms for the adsorption from the dry state and the desorption from w_{sat} and w_{cap} have been successfully obtained on untreated samples. For treated samples, the desorption curves starting from w_{sat} are also available. As demonstrated, the corresponding moisture contents approach or even overlap with each other, indicating that lime mortar does not have an obvious hysteresis phenomenon, and that hydrophobization causes a decrease in its hygroscopicity but only to a limited extent, whatever the agent concentration is.

The moisture retention curves obtained from the pressure plate tests are illustrated in Fig. 5. Clearly, the retention curves of untreated lime mortar decline slowly with the capillary pressure (p_c , Pa), while untreated ceramic brick and sintered glass have their curves rapidly decreased close to $p_c = 0$ Pa. These differences can be easily explained by the three materials' respective pore sizes.

For treated samples, the pressure plate method fails to produce reliable results. For ceramic brick and sintered glass, the moisture contents of treated samples are greater than the values of untreated ones, which is unreasonable. The main reason could be that after hydrophobization the hydraulic contact between samples and the ceramic plate in the pressure plate setup can no longer be perfectly maintained. For the same reason, the results of treated lime mortar are also questionable. From a scientific point of view, further investigations into the moisture retention characteristics of hydrophobized materials are therefore needed in the future. However, the necessity of such properties is on the other hand also debatable from an application perspective, as in practice these hydrophobized materials are unlikely to absorb much liquid water or to go through the desorption process in the over-hygroscopic range.

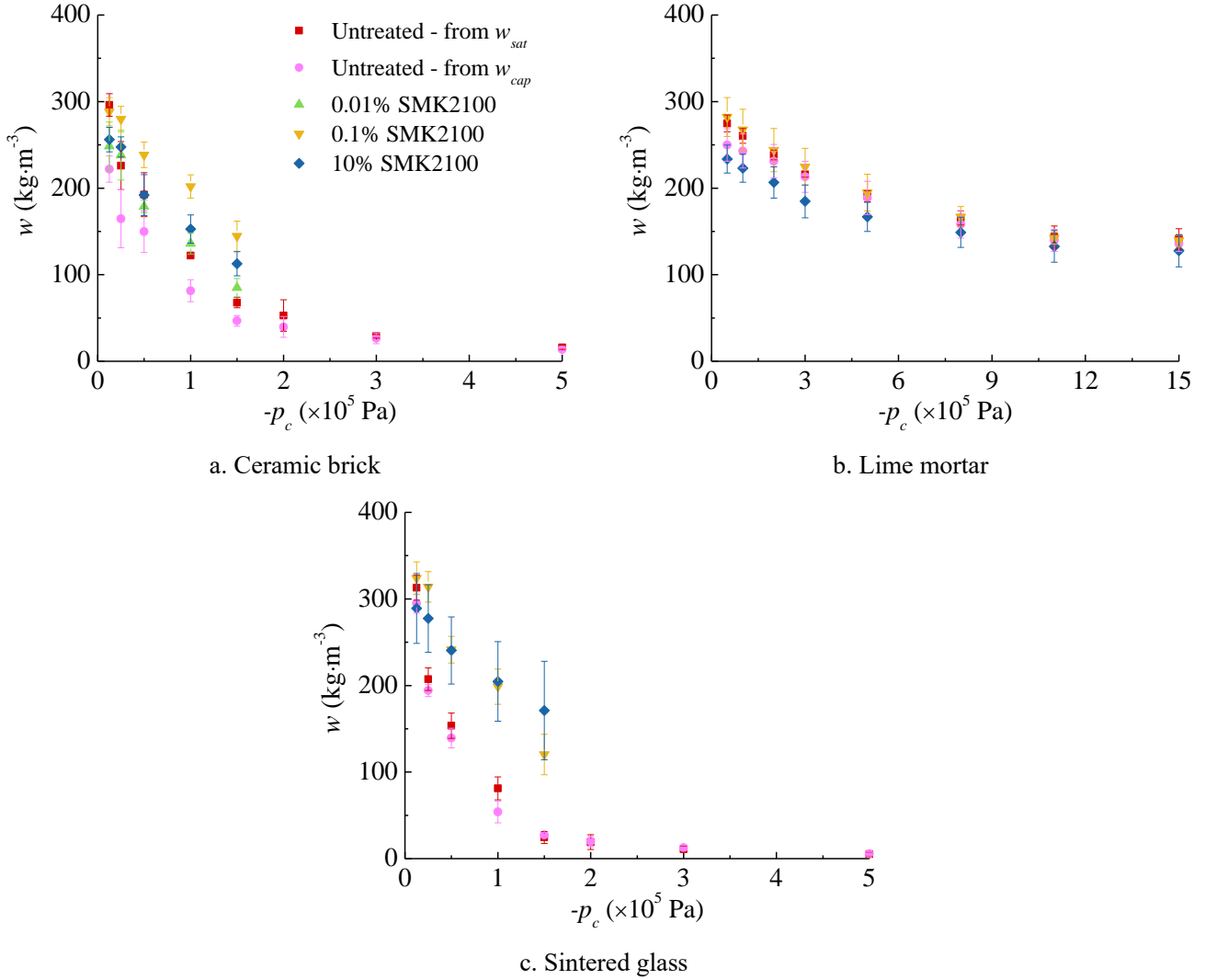


Fig. 5 The moisture retention curves obtained from the pressure plate tests

3.3 Results from moisture transport tests

The capillary absorption coefficients obtained from the capillary absorption tests are illustrated in Fig. 6. Obviously, hydrophobization reduces capillary absorption: the higher the agent concentration is, the lower the A_{cap} values become. Interestingly, the critical agent concentration comes into being, beyond which a sharp decrease in A_{cap} occurs. For lime mortar this threshold is between 0.1% and 10%, while for ceramic brick and sintered glass it is below 0.1%. Moreover, when treated at the same agent concentrations, lime mortar always suffers from the smallest impact, followed by ceramic brick and then by sintered glass. These phenomena may result from the pore sizes of different materials, which is discussed in Section 4 more specifically.

As explained before, the capillary moisture content of treated samples cannot always be obtained: if the capillary absorption coefficient is very small after hydrophobization, then the water front does not (easily) reach the sample's top. For all successful cases, the results are listed in Table 3. It should be kept in mind that these are also the cases where hydrophobization is performed below the critical concentration, agreeing with the results in Fig. 6. In fact, in a trial capillary absorption test brick samples ($4\times 4\times 0.2$ cm^3 , treated by 10% SMK2100) merely reached moisture contents around $40\sim 50$ $\text{kg}\cdot\text{m}^{-3}$ after almost a whole year, much lower than the value for untreated samples. On the contrary,

some researchers reported a w_{cap} reduction merely by 20%~30% on other materials treated by another agent [20]. It is therefore difficult to evaluate the impact of hydrophobization on w_{cap} .

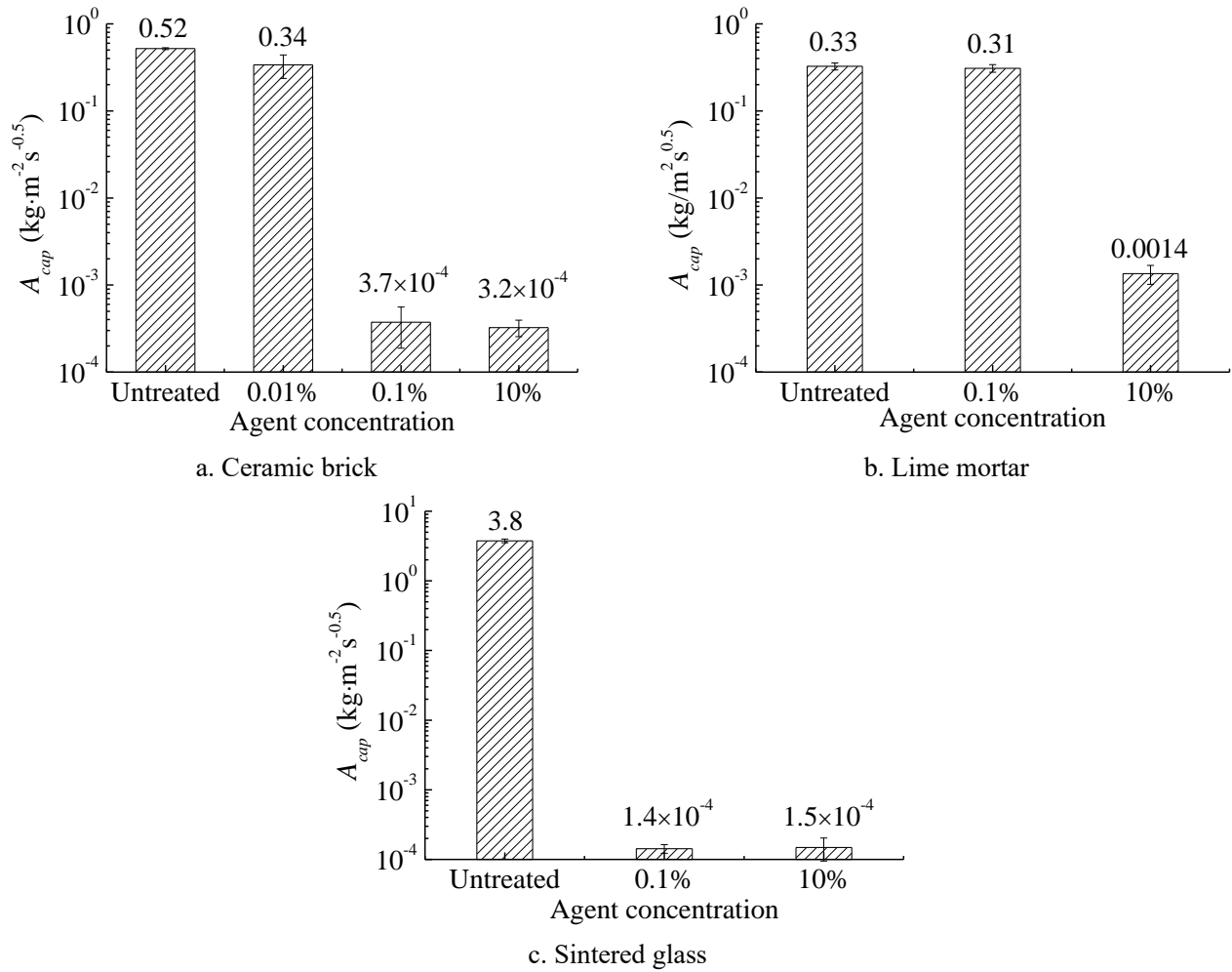


Fig. 6 The capillary absorption setup and the capillary absorption coefficients

Table 3 The capillary moisture contents obtained from the capillary absorption tests

Material	Agent concentration	w_{cap} ($\text{kg}\cdot\text{m}^{-3}$)	
		Average	Standard deviation
Ceramic brick	Untreated	197	7
	0.01%	199	8
Lime mortar	Untreated	268	5
	0.1%	262	5

The liquid permeability obtained from the falling-head water column test is illustrated in Fig. 7. As references, the w_{sat} and w_{cap} values of untreated materials are indicated. A common phenomenon can be observed that the liquid permeability increases with the moisture content. This is what can be expected from the basic principles for liquid transfer [46]. When it comes to the impact of hydrophobization, it can be observed that higher agent concentrations yield lower K_l values. To explain this, we should keep in mind that in this moisture regime, capillary forces no longer play a dominant role. Therefore, the changes in the contact angle due to the hydrophobization treatment should not be

blamed. A more reasonable explanation is that the fixation of the water repellent agent on the surfaces of pores throughout the sample (especially the small pores) partially blocks pathways for water movement so that the K_l values are reduced.

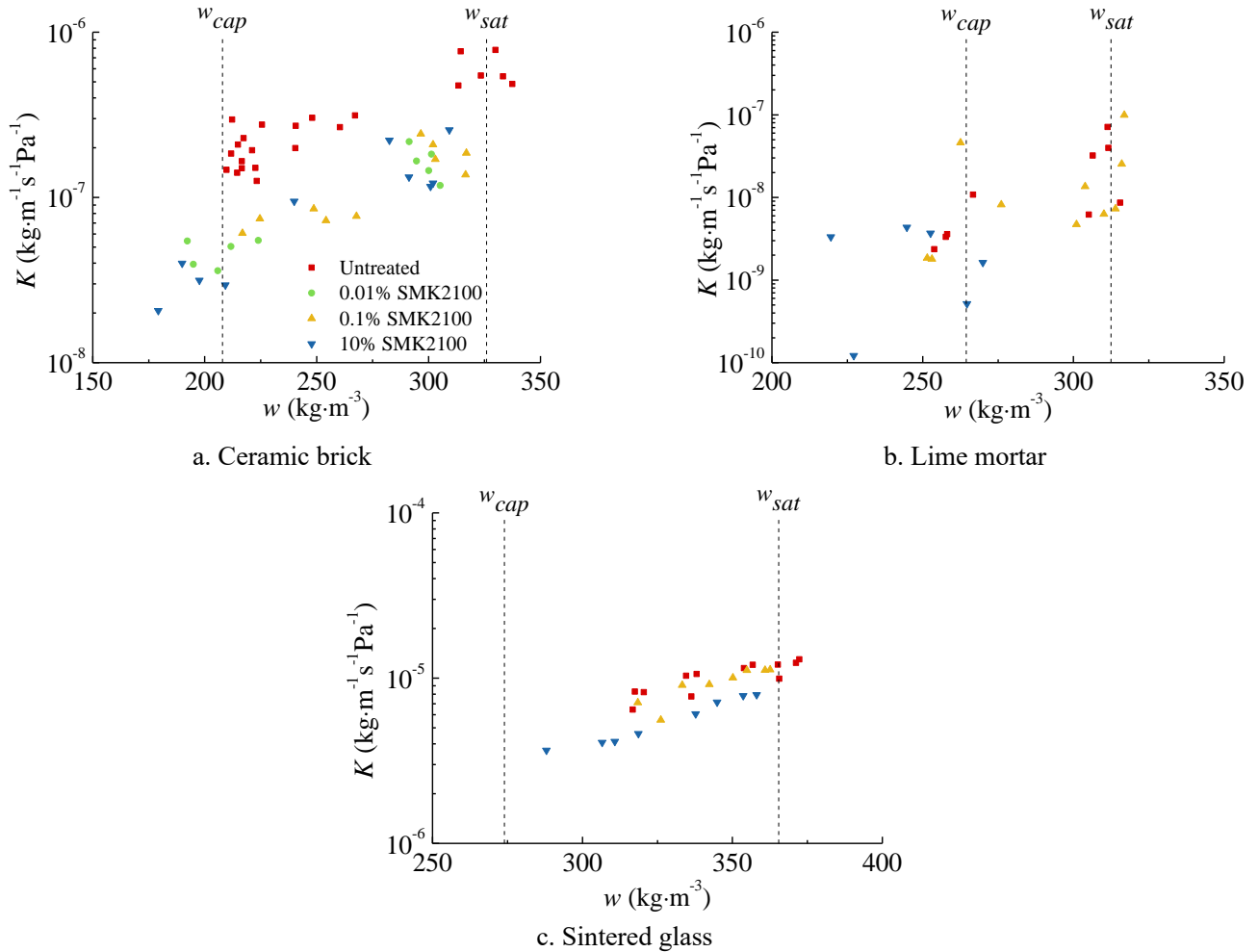


Fig. 7 The liquid permeabilities obtained from the falling-head water column tests.

The vapor diffusion resistance factors obtained from the cup tests are illustrated in Fig. 8, revealing two trends. First, the μ value decreases as the RH increases. This can be expected due to the capillary condensation and its resulting transport facilitation, as reflected by numerous cup tests [47, 48]. This effect is weaker in brick, due to its larger pore size and the resultantly weaker hygroscopicity. More importantly, the μ value increases with the concentration of the water repellent agent, agreeing with other reported measurements [49]. This reflects the rising impact of hydrophobization, which increases the contact angle and hence delays the capillary condensation and its resulting transport facilitation.

It should be remarked that for ceramic brick untreated samples are also tested at RH 53.5%~84.7%, yielding a μ value of 11.1 ± 1.0 . The measurements at these RH conditions are not performed for treated bricks, as these results would not add much value. It should also be mentioned that sintered glass has a larger pore size than ceramic brick, and is hence even less hygroscopic. Consequently, the hydrophobization treatment should have a very limited effect on its vapor diffusion, and the measurements on sintered glass samples are thus not carried out.

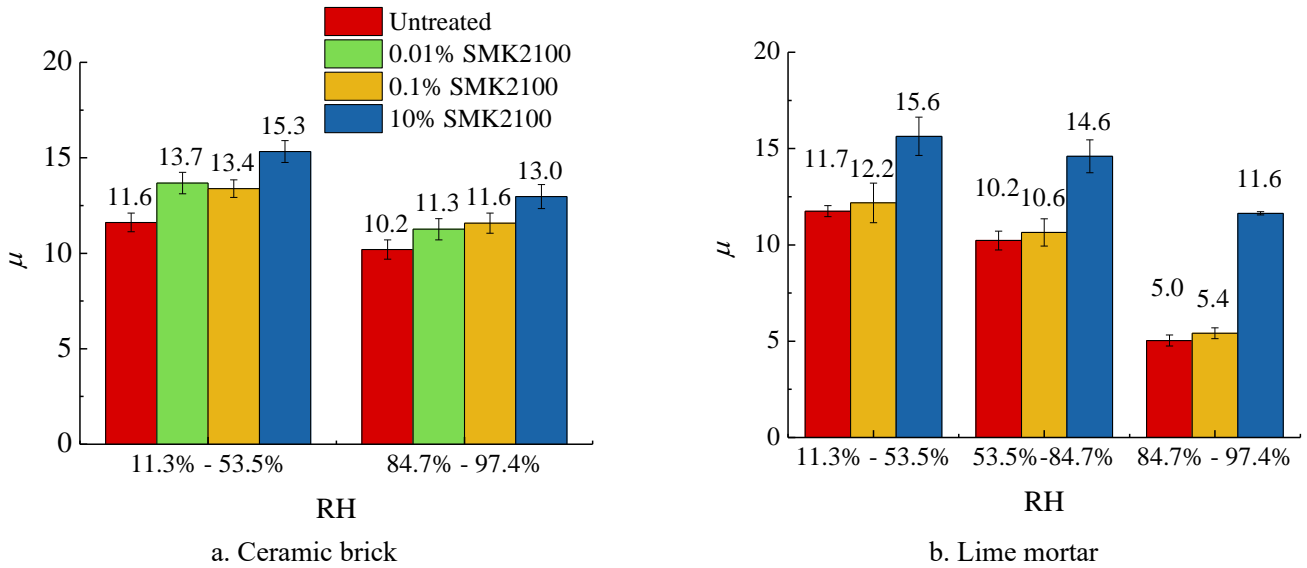


Fig. 8 The vapor diffusion resistance factors obtained from the cup tests

The equivalent moisture transport resistance factors obtained from the drying tests are illustrated in Fig. 9, with the vapor diffusion resistance factors from Fig. 8 indicated as reference. Clearly, when the samples are untreated or treated below the critical agent concentration, the μ values measured from the drying tests are much lower than the values from the cup test. Actually, these μ values from the drying tests are even smaller than 1, meaning that the resistance is smaller than stagnant air. This is a clear indication that liquid transport plays an important role. On the contrary, when the samples are treated above the critical agent concentration, the μ values measured from the drying tests become comparable with the values from the cup tests. This indicates that liquid transport no longer plays a significant role, and now it is vapor diffusion that dominates.

From the moisture transport tests, it can be summarized that there is a critical concentration of the hydrophobization agent, with varied values for different materials. When a material is treated above this concentration, its capillarity is significantly reduced. In the hygroscopic range however, pure vapor diffusion is not severely influenced.

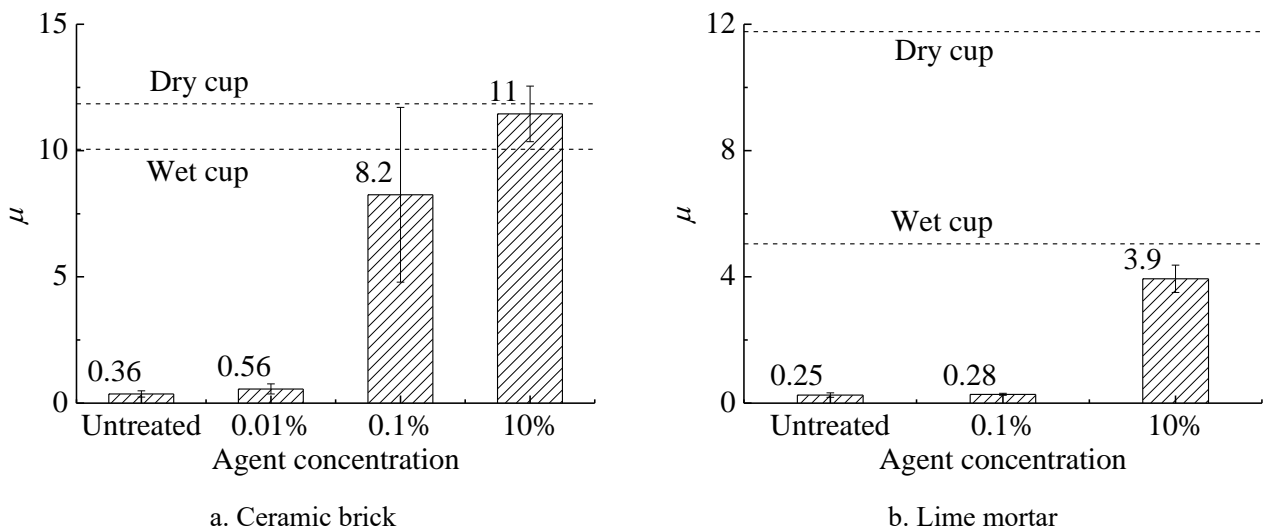


Fig. 9 The equivalent moisture transport resistance factors obtained from the drying tests

4. Discussion

4.1 Comparison with other studies

This research investigates the impact of hydrophobization on the hygric properties of porous building material. To have a wider perspective, we confront our experimental results with other quantitative reports summarized in Table 4.

Table 4 Impact of hydrophobization of moisture transport

Researcher	Material	Agent type	Main results
Hansen et al [12]	Brick and lime mortar	16 different agents	μ decreases by 4%~9% for brick and 0%~29% for mortar; moisture content after 20-h immersion fluctuates.
Klisińska-Kopacz and Tišlova [17]	Roman cement mortar	3 different agents	A_{cap} decreases by 61%~85%.
MacMullen et al [19]	Brick and mortar	Polymer cream	Moisture content after 24-h immersion decreases by 97% for brick, 85% for one mortar and 22% for another mortar.
Carmeliet et al [20]	Ceramic brick and calcium silicate brick	Alkyl-alkoxysilane	A_{cap} decreases by a factor of 290 for ceramic brick and by 97% for calcium silicate brick; μ increases by a factor of 2 for ceramic brick and 6 for calcium silicate brick.
MacMullen et al [21]	Brick	Silane/siloxane emulsion	A_{cap} decreases by 88%~92%; μ increases by 92%~150%.
Zhao and Meissener [26]	Historic building brick	Silicone-based	A_{cap} decreases by a factor of 50; μ decreases within 13%; a higher agent concentration had a greater impact.
Vejmelková et al [49]	Lime-metakaolin plaster	Zinc stearate	A_{cap} decreases by 72%~99%; μ decreases by 13%~39% (dry cup) and 25%~53% (wet cup).
This study	Ceramic brick, lime mortar and sintered glass	Mixture of silanes and siloxanes	A_{cap} decreases by a factor up to 1600 for brick, 240 for mortar and 27000 for sintered glass; μ increases by 11%~32% for brick and 4%~132% for mortar.

To start with, Table 4 demonstrates a contradiction in vapor transport. Unlike the majority of other researchers, Hansen et al [12], Zhao and Meissener [26] and Vejmelková et al [49] reported enhanced vapor transport after hydrophobization, which is physically unreasonable. The former two studies attributed their irregularities to experimental uncertainties, while the last one found an explanation from their operational procedure – the water repellent agent was added to the fresh plaster mixture before hardening, leading to an increased open porosity afterward. This indicates that treatment protocols also play an important role in applying hydrophobization.

By excluding the above-mentioned abnormal observations, we can easily summarize that our results are in overall consistency with reported studies, even if the specific materials and water repellent agents are different. Two trends can be further generalized. For one thing, hydrophobization has a significant reduction in liquid water transport, while the reduction of vapor transport is much more moderate. For another thing, bricks suffer from a greater impact on the capillarity than mortars do, while the opposite is true for vapor transport. Both trends can be explained by the pore sizes of different materials.

4.2 The roles of pore size

In the over-hygroscopic range where liquid dominates, the large pores play a central role. Once these

pore surfaces are covered by the water repellent agent, the material loses its capillarity so that its capillary absorption is significantly reduced. Such surface coverage does not impact the Fickian diffusion of water vapor obviously except for the reduced transport pathways, thus the impact on vapor transport is much more moderate (Fig. 8), similar to the water head tests measuring Darcy's flow (Fig. 7). However, water repellent agents typically have large molecules. It is therefore difficult for them to penetrate into the very fine pores of porous building materials, and some minor capillarity can be retained [20]. This explains the phenomenon in Fig. 6 and Table 4 that mortar (with a smaller pore size) suffers from less A_{cap} reduction than ceramic brick and sintered glass (with larger pore sizes), and the phenomenon in Fig. 9 that mortar has a smaller equivalent moisture transport resistance factor in the drying test. Moreover, the penetration difficulty means that these small pores – which are most responsible for hygroscopic sorption as they have the largest pore surfaces and easiest capillary condensation – can keep their hygroscopicity almost intact. This is the reason why the sorption isotherms of lime mortar in Fig. 4 are only slightly lowered after hydrophobization.

Besides the easiness for water repellent agents to penetrate, the pore size can influence the effectiveness of hydrophobization via the pore surface area. As is clearly shown in Fig. 6, the same agent concentration produces the least impact on lime mortar and the greatest impact on sintered glass. An additional explanation can therefore be found in the ratio of the agent amount versus the pore surface area. Fig. 2 demonstrates that the open porosities for all three target materials are similar, meaning that almost the same amount of diluted agent is absorbed by the material when treated at the same concentration. However, the smaller pore size of lime mortar indicates a much larger pore surface area. Consequently, the agent amounts adequate to cover all (or most of) the pore surfaces of ceramic brick and sintered glass may fail to provide enough coverage to lime mortar, resulting in its less reduced capillarity. Lubelli and van Hees [22] also suggested that the amount of agent applied to a material should depend on its porosity and pore size distribution, supporting our explanation. All these imply a threshold concentration, beyond which the agent starts to display its effectiveness obviously.

4.3 The critical agent concentration

Numerous measurements show that water repellent agents increase the contact angle between water molecules and pore surfaces of building materials from the normally assumed 0° for untreated materials to $100^\circ\sim 140^\circ$ after hydrophobization [19, 21, 50, 51]. As a result, the spontaneous water absorption no longer occurs. This explains how hydrophobization is physically realized, and it also implies that the pore surfaces must be covered by the molecules of water repellent agents for effectiveness.

When a material is untreated, the coverage of its pore surfaces is 0; when the coverage ratio is 100%, the maximum water repellent effect is achieved. By analogy with the concept of the critical moisture content in building physics (referring to the moisture content at which the liquid phase in a material is continuous), we can define a critical coverage above which the liquid phase in a hydrophobized material can no longer maintain continuity, so that the material loses most of its capillarity and vapor diffusion becomes the sole transport mechanism. With a specific treatment method, the critical concentration of the water repellent agent can be further defined. Fig. 10 illustrates the concept.

It is straightforward that the critical agent concentration depends on several factors, such as the features of the material, the type of the water repellent agent, as well as the protocol of implementing hydrophobization. It can also be expected that hydrophobization far beyond the critical agent concentration does not necessarily guarantee a thorough water repellent effect, especially when a material has very fine pores. Similar to the critical moisture content, the critical agent concentration is

clear in physical interpretation but not easy in experimental determination. However, its estimation already provides great value. Taking this study as an example, we can expect (with over-estimations) a critical concentration of 10% for lime mortar and 0.1% for ceramic brick when treated with the SMK2100 agent according to our protocol. The fact that the critical concentration for ceramic brick is much lower than the producer’s 10% recommendation implies that a much better compromise between economy and effectiveness can be reached.

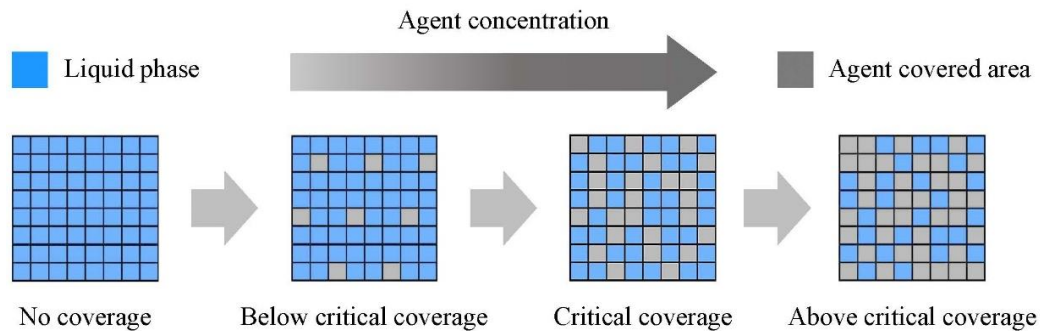


Fig. 10 The concept of critical coverage/concentration

5. Conclusions

This study examines the effect of hydrophobization to porous building materials. We propose a novel concept of a material-dependent critical agent concentration: the lowest concentration that ensures hydrophobic effectiveness on a specific material. To prove its validity, eight tests are performed on ceramic brick, lime mortar and sintered glass to obtain their basic, moisture storage and moisture transport properties. Based on extensive measurements and thorough analysis, hydrophobization demonstrates the greatest impact on sintered glass, followed by ceramic brick and lime mortar in sequence. More importantly, the following general conclusions can be drawn:

- The effectiveness of hydrophobization depends on materials’ pore sizes and the imposed agent amounts. There is a material-dependent critical concentration of the water repellent agent, beyond which the impact of hydrophobization becomes clear;
- When a material is treated above the critical agent concentration, its capillarity is significantly influenced, while its hygroscopicity is moderately reduced;
- Hydrophobization has a limited impact on a material’s bulk density, open porosity and pore size distribution, although small pores may get partially blocked.

It should be kept in mind though that these impacts of hydrophobization strongly depend on the interaction between water repellent agent and material pore structure, and that these outcomes should only cautiously be generalized.

Acknowledgements

This research is supported by Key Laboratory of New Technology for Construction of Cities in Mountain Area (Project No. LNTCCMA-20200108) and EU H2020 project “RIBuild - Robust Internal Thermal Insulation of Historic Buildings” (No. 637268). We also thank WACKER Chemical Corporation for providing the hydrophobization agent.

References

- [1] <https://www.iea.org/statistics/balances/>.
- [2] D. Ürge-Vorsatz, L.F. Cabeza, S. Serrano, C. Barreneche, K. Petrichenko, Heating and cooling energy trends and drivers in buildings, *Renewable and Sustainable Energy Reviews* 41 (2015) 85-98.
- [3] L. Frayssinet, L. Merlier, F. Kuznik, J.-L. Hubert, M. Milliez, J.-J. Roux, Modeling the heating and cooling energy demand of urban buildings at city scale, *Renewable and Sustainable Energy Reviews* 81 (2018) 2318-2327.
- [4] H. Fu, Y. Ding, M. Li, H. Li, X. Huang, Z. Wang, Research on thermal performance and hygrothermal behavior of timber-framed walls with different external insulation layer: Insulation Cork Board and anti-corrosion pine plate, *Journal of Building Engineering* 28 (2020) 101069.
- [5] M. Pedroso, I. Flores-Colen, J.D. Silvestre, M.G. Gomes, L. Silva, P. Sequeira, J. de Brito, Characterisation of a multilayer external wall thermal insulation system. Application in a Mediterranean climate, *Journal of Building Engineering* 30 (2020) 101265.
- [6] E. Lucchi, F. Becherini, M.C. Di Tuccio, A. Troi, J. Frick, F. Roberti, C. Hermann, I. Fairnington, G. Mezzasalma, L. Pockelé, A. Bernardi, Thermal performance evaluation and comfort assessment of advanced aerogel as blown-in insulation for historic buildings, *Building and Environment* 122 (2017) 258-268.
- [7] V. Murgul, V. Pukhkal, Saving the Architectural Appearance of the Historical Buildings due to Heat Insulation of their External Walls, *Procedia Engineering* 117 (2015) 891-899.
- [8] E. Vereecken, L. Van Gelder, H. Janssen, S. Roels, Interior insulation for wall retrofitting – A probabilistic analysis of energy savings and hygrothermal risks, *Energy and Buildings* 89 (2015) 231-244.
- [9] X. Zhou, D. Derome, J. Carmeliet, Hygrothermal modeling and evaluation of freeze-thaw damage risk of masonry walls retrofitted with internal insulation, *Building and Environment* 125 (2017) 285-298.
- [10] L. Havinga, H. Schellen, Applying internal insulation in post-war prefab housing: Understanding and mitigating the hygrothermal risks, *Building and Environment* 144 (2018) 631-647.
- [11] L. Havinga, H. Schellen, The impact of convective vapour transport on the hygrothermal risk of the internal insulation of post-war lightweight prefab housing, *Energy and Buildings* 204 (2019) 109418.
- [12] T.K. Hansen, S.P. Bjarløv, R.H. Peuhkuri, K.K. Hansen, Performance of hydrophobized historic solid masonry – Experimental approach, *Construction and Building Materials* 188 (2018) 695-708.
- [13] G.R. Finken, S.P. Bjarløv, R.H. Peuhkuri, Effect of façade impregnation on feasibility of capillary active thermal internal insulation for a historic dormitory – A hygrothermal simulation study, *Construction and Building Materials* 113 (2016) 202-214.
- [14] T.K. Hansen, S.P. Bjarløv, R. Peuhkuri, The effects of wind-driven rain on the hygrothermal conditions behind wooden beam ends and at the interfaces between internal insulation and existing solid masonry, *Energy and Buildings* 196 (2019) 255-268.
- [15] L. Veelaert, E. Du Bois, I. Moons, E. Karana, Experiential characterization of materials in product design: A literature review, *Materials & Design* 190 (2020) 108543.
- [16] A.A. Morini, M.J. Ribeiro, D. Hotza, Early-stage materials selection based on embodied energy and carbon footprint, *Materials & Design* 178 (2019) 107861.
- [17] A. Klisińska-Kopacz, R. Tišlova, Effect of hydrophobization treatment on the hydration of repair Roman cement mortars, *Construction and Building Materials* 35 (2012) 735-740.
- [18] A.E. Charola, Water-Repellent Treatments for Building Stones: A Practical Overview, *APT Bulletin* 26(2/3) (1995) 10-17.
- [19] J. MacMullen, Z. Zhang, E. Rirsch, H.N. Dhakal, N. Bennett, Brick and mortar treatment by cream emulsion for improved water repellence and thermal insulation, *Energy and Buildings* 43(7) (2011) 1560-1565.
- [20] J. Carmeliet, G. Houvenaghel, J.v. Schijndel, S. Roels, Moisture phenomena in hydrophobic porous building material

Part 1: Measurements and physical interpretations, *Restoration of Buildings and Monuments* 8(2-3) (2002) 165-184.

- [21] J. MacMullen, Z. Zhang, J. Radulovic, C. Herodotou, M. Totomis, H.N. Dhakal, N. Bennett, Titanium dioxide and zinc oxide nano-particulate enhanced oil-in-water (O/W) facade emulsions for improved masonry thermal insulation and protection, *Energy and Buildings* 52 (2012) 86-92.
- [22] B. Lubelli, R. van Hees, Evaluation of the Effect of Nano-Coatings with Water Repellent Properties on the Absorption and Drying Behaviour of Brick, 6th International Conference on Water Repellent Treatment of Building Materials; Aedificatio Publishers: Freiburg, Germany, 2011, pp. 125-136.
- [23] V. Soulios, E. Jan de Place Hansen, C. Feng, H. Janssen, Hygric behavior of hydrophobized brick and mortar samples, *Building and Environment* 176 (2020) 106843.
- [24] H. Mayer, Masonry protection with silanes, siloxanes and silicone resins, *Surface coatings international* 81(2) (1998) 89-93.
- [25] J. Engel, P. Heinze, R. Plagge, Adapting hydrophobizing impregnation agents to the object, *Restoration of Buildings and Monuments* 20(6) (2014) 433-440.
- [26] J. Zhao, F. Meissener, Experimental investigation of moisture properties of historic building material with hydrophobization treatment, *Energy Procedia* 132 (2017) 261-266.
- [27] <https://www.vandersandengroup.com/bricks/en/brick-brickslip/robusta>.
- [28] <http://www.stastier.co.uk/nhl/data/nhl35.htm>.
- [29] <https://www.robuglas.com/en/service/poresizes.html>.
- [30] <https://www.wacker.com/cms/en-us/products/brands/silres/silres.html>.
- [31] ISO 10545-3: 2018 (E) Ceramic tiles - Part 3: Determination of water absorption, apparent porosity, apparent relative density and bulk density, 2018.
- [32] ASTM D4404 - 18: Standard Test Method for Determination of Pore Volume and Pore Volume Distribution of Soil and Rock by Mercury Intrusion Porosimetry, 2018.
- [33] ISO 12571: 2013(E) Hygrothermal performance of building materials and products - Determination of hygroscopic sorption properties, 2013.
- [34] ASTM C1699 - 09 (Reapproved 2015): Standard Test Method for Moisture Retention Curves of Porous Building Materials Using Pressure Plates, 2015.
- [35] ASTM C1794 - 15: Standard Test Methods for Determination of the Water Absorption Coefficient by Partial Immersion, 2015.
- [36] ISO 17892-11: 2019(E) Geotechnical investigation and testing - Laboratory testing of soil - Part 11: Permeability tests, 2019.
- [37] ISO 12572: 2016(E) Hygrothermal performance of building materials and products - Determination of water vapour transmission properties - Cup method, 2016.
- [38] S. Diamond, Mercury porosimetry: an inappropriate method for the measurement of pore size distributions in cement-based materials, *Cement and Concrete Research* 30(10) (2000) 1517-1525.
- [39] R.A. Cook, K.C. Hover, Mercury porosimetry of cement-based materials and associated correction factors, *Construction and Building Materials* 7(4) (1993) 231-240.
- [40] R.J. Good, R.S. Mikhail, The contact angle in mercury intrusion porosimetry, *Powder Technology* 29(1) (1981) 53-62.
- [41] G.F.B. Sandoval, I. Galobardes, R.S. Teixeira, B.M. Toralles, Comparison between the falling head and the constant head permeability tests to assess the permeability coefficient of sustainable Pervious Concretes, *Case Studies in Construction Materials* 7 (2017) 317-328.
- [42] J.J. Nijp, K. Metselaar, J. Limpens, H.P.A. Gooren, S.E.A.T.M. van der Zee, A modification of the constant-head permeameter to measure saturated hydraulic conductivity of highly permeable media, *MethodsX* 4 (2017) 134-142.
- [43] A. Pedescoll, R. Samsó, E. Romero, J. Puigagut, J. García, Reliability, repeatability and accuracy of the falling head

method for hydraulic conductivity measurements under laboratory conditions, *Ecological Engineering* 37(5) (2011) 754-757.

[44] R. Cardoso, Influence of Water–Cement Ratio on the Hydraulic Behavior of an Artificially Cemented Sand, *Geotechnical and Geological Engineering* 35(4) (2017) 1513-1527.

[45] H. Alghamdi, A. Dakhane, A. Alum, M. Abbaszadegan, B. Mobasher, N. Neithalath, Synthesis and characterization of economical, multi-functional porous ceramics based on abundant aluminosilicates, *Materials & Design* 152 (2018) 10-21.

[46] J. Carmeliet, H. Hens, S. Roels, O. Adan, H. Brocken, R. Cerny, Z. Pavlik, C. Hall, K. Kumaran, L. Pel, Determination of the liquid water diffusivity from transient moisture transfer experiments, *Journal of Thermal Envelope and Building Science* 27(4) (2004) 277-305.

[47] C. Feng, H. Janssen, Y. Feng, Q. Meng, Hygric properties of porous building materials: Analysis of measurement repeatability and reproducibility, *Building and Environment* 85 (2015) 160-172.

[48] C. Feng, H. Janssen, Hygric properties of porous building materials (II): Analysis of temperature influence, *Building and Environment* 99 (2016) 107-118.

[49] E. Vejmelková, D. Koňáková, M. Čáchová, M. Keppert, R. Černý, Effect of hydrophobization on the properties of lime–metakaolin plasters, *Construction and Building Materials* 37 (2012) 556-561.

[50] T. van Besien, S. Roels, J. Carmeliet, A laboratory study of the efficiency of a hydrophobic treatment of cracked porous building materials, *Research in Building Physics: Proceedings of the Second International Conference on Building Physics*, Leuven, Belgium, 14-18 September 2003, CRC Press, 2003, p. 301.

[51] K. Sandin, Influence of cracks on moisture conditions in facades with water-repellent treatments/Einfluss von Rissen auf den Feuchtigkeitshaushalt hydrophobierter Fassaden, *Restoration of Buildings and Monuments* 5(5) (1999) 499-522.

Appendix: Calculation of liquid permeability (K_l) from the falling-head test

In the falling-head water column test (Fig. A-1), upward is defined as the positive direction. Assume a water column with a changing height H (m) and a constant intersection area S (m²), then within time interval dt (s) the total flow volume dV (m³) is:

$$dV = -S \cdot dH(t) \quad (\text{A-1})$$

The mass flow rate \dot{G} (kg·s⁻¹) is therefore:

$$\dot{G} = \rho_{water} \cdot \frac{dV}{dt} = -\rho_{water} \cdot S \cdot \frac{dH(t)}{dt} \quad (\text{A-2})$$

where ρ_{water} is the water density, kg·m⁻³.

The sample's surface area is A (m²), its thickness is T (m). According to Darcy's law, the water flux \dot{g} (kg·m⁻²·s⁻¹) through the sample can be written as:

$$\dot{g} = K_l \cdot \frac{\Delta p_l}{T} = K_l \cdot \frac{\rho_{water} \cdot g \cdot H(t)}{T} \quad (\text{A-3})$$

where Δp_l is the liquid pressure difference (Pa) and g the gravitational acceleration (m·s⁻²).

The water flow \dot{G} through the sample is therefore:

$$\dot{G} = \dot{g} \cdot A = K_l \cdot \frac{A \cdot \rho_{water} \cdot g}{T} \cdot H(t) \quad (\text{A-4})$$

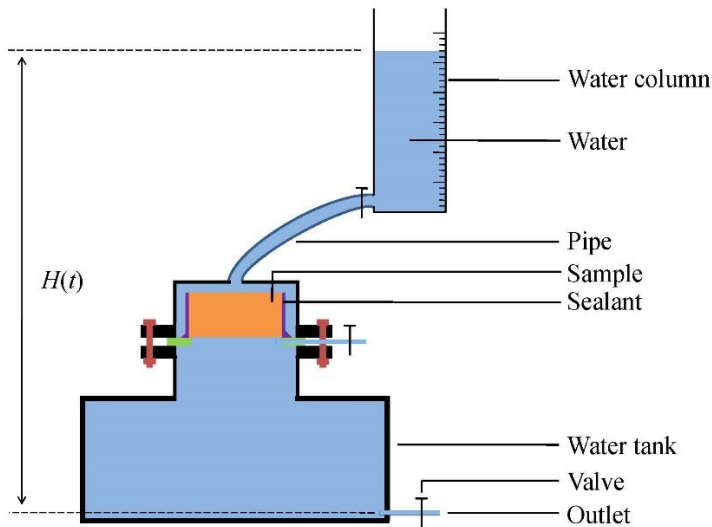
Equating Eq.(A-2) and (A-4) yields:

$$-\rho_{water} \cdot S \cdot \frac{dH(t)}{dt} = K_l \cdot \frac{A \cdot \rho_{water} \cdot g}{T} \cdot H(t) \quad (\text{A-5})$$

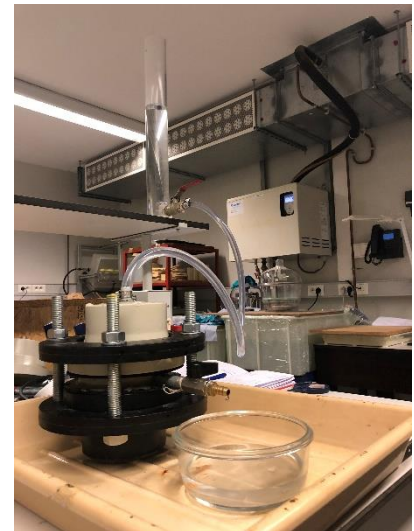
which finally gives the solution:

$$\ln H(t) = -K_l \cdot \frac{A \cdot g}{S \cdot T} \cdot t + \ln H_{t=0} \quad (\text{A-6})$$

The liquid permeability K_l can thus be obtained.



a. A schematic



b. A photo

Fig. A-1 The falling-head water column setup